# Electron-hole scattering in GaAs quantum wells

R. A. Höpfel
*Institut für Experimentalphysik, Universität Innsbruck, Technikerstrasse 25, A-6020 Innsbruck, Austria*

J. Shah
*AT&T Bell Laboratories, Holmdel, New Jersey 07733-1988*

P. A. Wolff
*Francis Bitter National Magnet Laboratory, Massachusetts Institute of Technology, Cambridge, Massachusetts 02139*

A. C. Gossard
*AT&T Bell Laboratories, Murray Hill, New Jersey 07974-2070*
(Received 14 July 1987)

Momentum and energy relaxation of minority carriers in GaAs quantum wells is studied in a series of experiments. At low temperatures electron-hole scattering is the dominant scattering mechanism for minority carriers in high-quality samples, causing dramatic carrier-drag effects (e.g., negative drift or negative absolute mobility) in the minority-carrier transport. Quantitative analysis of all-optical drift-velocity measurements shows that the momentum relaxation times of minority electrons in a hole plasma are much shorter (40–100 fs) than those of minority holes in an electron plasma (2–5 ps). Besides the different effective masses, part of this large difference is due to degeneracy of the electron plasma and due to effects from two dimensionality. At high electric fields, energy transfer between electrons and holes in the nonequilibrium plasma is studied. Characteristic transfer times of 200–500 fs (temperature dependent) are determined from simultaneous measurements of minority-electron energy-loss and energy distribution.

## I. INTRODUCTION

Minority-carrier drift in semiconductors was first studied in the historic experiments of Haynes and Shockley.[1] In these and similar subsequent experiments[2] the dynamics of minority electrons and holes were mainly determined by the scattering processes with impurities and phonons, by diffusion and by recombination processes. The main role of the majority-carrier plasma in these experiments was to screen the space charge of the injected minority carriers. Scattering *between* the two types of carriers was taken into account first by Paige[3] after measuring the minority-carrier drift in Ge at low temperatures. In a subsequent paper,[4] McLean and Paige presented a detailed theory of the effects of electron-hole scattering on the mobility. For strong electron-hole scattering and weak carrier-lattice scattering, they predicted negative mobility of minority carriers due to the "carrier drag" (momentum transfer) of the drifting majority-carrier plasma via electron-hole scattering. In the special case of holes in $n$-type InSb, the momentum transfer from the drifting high-mobility electrons was predicted to be strong enough to drag the minority holes in the "wrong" direction towards the positive electrode. Since then, several experimental works have been reported on the influence of electron-hole scattering and carrier drag on minority-carrier mobility.[5–12] However, negative absolute mobility could never be observed in bulk semiconductor crystals.[13,14] As it will be shown later, high mobility and high carrier density are necessary for negative mobility, which is not possible to achieve in bulk semiconductors, due to impurity scattering.

Recently, we were able to observe the effect of negative absolute mobility for both minority electrons and minority holes in "modulation-doped" GaAs quantum wells.[15,16] In previous experiments[17] we measured the energy-loss rates and carrier temperatures in the case of strong electron-hole scattering. In this paper we present a detailed and quantitative analysis of these experiments. The main results can be summarized as follows.

(1) At low temperatures electron-hole scattering is the dominant scattering mechanism of minority electrons and minority holes—due to the high mobility *and* high density of the majority-carrier plasma in the quantum wells. The carrier-drag effect is strong enough to cause "negative absolute mobility"—minority electrons in a hole plasma are dragged towards the negative electrode, minority holes in an electron plasma drift towards the positive electrode.

(2) The momentum relaxation of minority electrons and minority holes differ—at comparable plasma densities by a factor of about 50. The different effective masses explain a linear factor of the mass ratio (about 6) through the classical mechanics of the momentum transfer by Coulomb collisions. The remaining difference is attributed partly to the degeneracy of the majority-electron plasma, to the more three-dimensional nature of our $n$-type samples and to different screening, which all leads to a strong reduction of the momentum relaxation of injected minority holes.

 

(3) The energy relaxation of minority electrons is enhanced by electron-hole scattering, which introduces an additional energy-loss mechanism. This energy-transfer rate is quantitatively determined as the difference of the total energy-loss rate and the energy loss through optical-phonon emission. Energy relaxation times of 200–500 fs are obtained above room temperature.

## II. EXPERIMENTS

The experiments for the measurement of the minority-carrier drift are explained in the following for the case of $p$-type modulation-doped quantum wells, where injected electrons are the minority carriers. The minority-electron drift velocity is measured by a new all-optical technique, which is based on the following principle: The luminescence from injected minority electrons is time and spatially resolved. Because of the high majority-hole concentration, luminescence only occurs where minority electrons are, so that the study of the luminescence gives information on the minority-carrier dynamics. The technique is illustrated in Fig. 1: Electrons are excited in the semiconductor hole plasma by a focused laser pulse (6-ps pulses from a synchronously pumped, mode-locked, cavity-dumped dye laser, Rhodamine-6G, $\lambda = 606$ nm, repetition rate 4 MHz). The magnified spatial image of the time-integrated luminescence is studied as a function of the applied electric field. As will be shown later, the local luminescence intensity is directly proportional to the local electron concentration. Therefore the luminescence image directly reflects the spatial distribution of the injected minority carriers with and without electric field. The temporal evolution of the luminescence intensity is separately measured by picosecond time-resolved techniques. Combining both measurements allows the experimental determination of very low drift velocities $v_d$, depending on the carrier lifetimes $\tau_{\rm rec}$ and the resolvable drift length $l_d$ ($v_d \tau_{\rm rec} \geq l_d$).[18] Other techniques, such as time-resolved measurements of the photocurrent[19] are disturbed by trapping effects at low temperatures.[20] The effects on photoconductivity will be discussed in detail in Sec. VI.

The analysis of the experiments is based on the linear relation between the local photoluminescence intensity from free-carrier band-to-band recombination and the local *minority*-carrier concentration.[21] For the case of a $p$-type semiconductor and weak injection of minority electrons ($n \ll p_0$), the time-integrated local luminescence intensity ("intensity profile") can be written as

$$\int I(x,t)dt \propto \int n(x - v_d t, t=0) f_I(t) dt \ , \qquad (1)$$

where $v_d$ is the drift velocity of electrons. Equation (1) follows from the bimolecular radiative recombination characteristics, $I(x,t) \propto n(x,t)p(x,t)$,[21] and is valid independent of frequency and electric field, which have only effects on the absolute factors contained in the proportionality. The minority-carrier concentration $n(x,t)$ is separated in Eq. (1) into a product of spatial and time dependence, with the function $f_I(t)$ as the time dependence of the minority-electron concentration (thus proportional to the time dependence of the luminescence intensity for weak injection). Figure 2 illustrates the time-integration process for a drifting and decaying (recombining) electron "packet." The profile of the time-integrated luminescence intensity $\int I(x,t)dt$ is given by Eq. (1), under the following—justified—assumptions: The drift velocity is homogeneous along the carrier "packet,"[22] diffusion is neglected,[23] and the time dependence of the luminescence intensity (minority-carrier concentration), $f_I(t)$, is also homogeneous along the carrier "packet."[24]

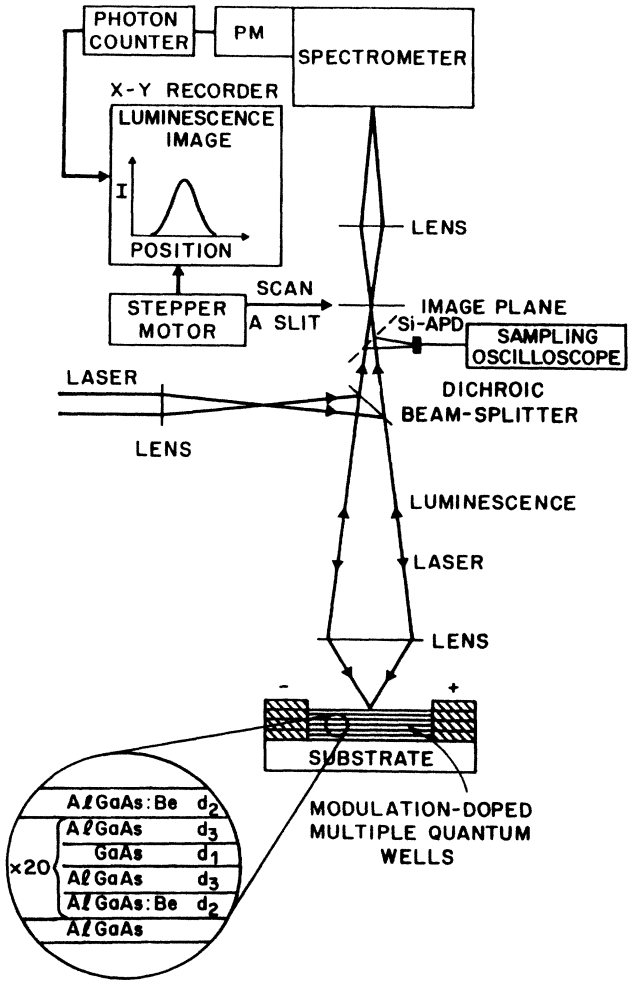


FIG. 1. Experimental setup for the measurement of minority drift velocities by spatially and time-resolved luminescence (luminescence "imaging").

The time dependence of the luminescence intensity, $f_I(t)$, is measured with a Si avalanche photodiode (APD), followed by a sampling oscilloscope (Tektronix S-4, 7T11, 7S11) and a signal averager. A time resolution of 440 ps [full width at half maximum (FWHM)] is obtained.

The spatial dependence of the luminescence (the luminescence "profile") is measured with an "imaging" technique. The laser beam is focused inside the cryostat down to a diameter of about 3 $\mu$m (using a Zeiss long-working-distance microscope objective). Through the same optics the photoluminescence is collected and magnified onto the "image plane" (Fig. 1). The magnified

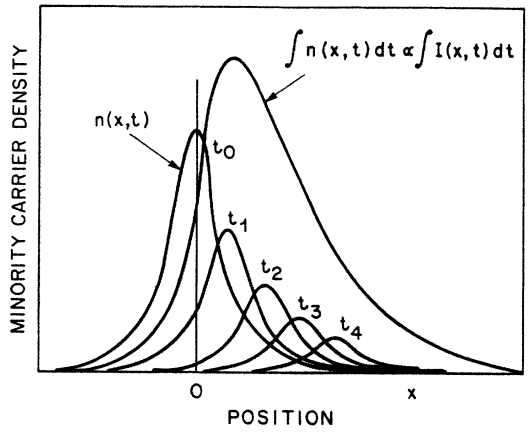


FIG. 2. Time integration of a drifting and decaying (recombining) carrier "packet." The local luminescence intensity is proportional to the local minority-carrier concentration.

luminescence image ($\times 13$) is scanned with a mechanical slit (width 25 $\mu$m), and spectrally analyzed to detect only the intrinsic band-to-band recombination. The luminescence spectra, as shown in Fig. 3, are characteristic of band-to-band recombination. For the spatially resolved ("imaging") experiment, the monochromator is set to the indicated wavelengths of maximum intensity, with a lower spectral resolution of about 10 nm.

The semiconductor structures in our experiments were $n$- or $p$-type modulation-doped multiple-quantum-well structures, grown by molecular-beam epitaxy.[25] The $p$-type sample has the following parameters: $d_1 = 112$ Å (GaAs), $d_2 = 49$ Å ($Al_{0.48}Ga_{0.52}As$ $p$ doped with Be), and $d_3 = 294$ Å (undoped $Al_xGa_{1-x}As$ "spacer layer"[25] between GaAs and doped $Al_xGa_{1-x}As$). This structure is repeated for 20 periods on a semi-insulating GaAs substrate. The hole mobilities and concentrations per GaAs layer are $p_0 = 1.5\times 10^{11}$ cm$^{-2}$, $\mu_p = 53\,800$ cm$^2$/V s (at 4.2 K), $p_0 = 1.8\times 10^{11}$ cm$^{-2}$, and $\mu_p = 3700$ cm$^2$/V s (at 77 K), determined by Hall measurements. Typical concentrations of injected minority carriers are $n \approx 3\times 10^{10}$ cm$^{-2}$ per layer, photoexcited by 6-ps laser pulses (wavelength 606 nm, repetition rate 4 MHz).

## III. RESULTS

The results on the time dependence of the luminescence are shown in Fig. 4: The inset shows the response of the Si-APD (dashed line) which can be easily measured with the scattered laser light from the sample. Using a cutoff filter, the time-dependent luminescence is detected (solid curve). The luminescence signal can be fitted very well by an exponential decay with *one* characteristic decay time. This is expected for minority injection and "bimolecular" recombination. The recombination time of minority electrons in the $p$-type sample is about 1.0 ns, almost independent of the lattice temperature (Fig. 4).

Figure 5 shows typical luminescence images for several lattice temperatures $T_L$. At the lowest temperature $T_L = 15$ K, without applied electric field, the image is symmetric [curve (a)]; with applied electric field [curve (b)] the image is shifted and distorted in the direction of the *minus* pole of the applied voltage. As temperature is increased, the drift becomes smaller [curve (c)], and be-

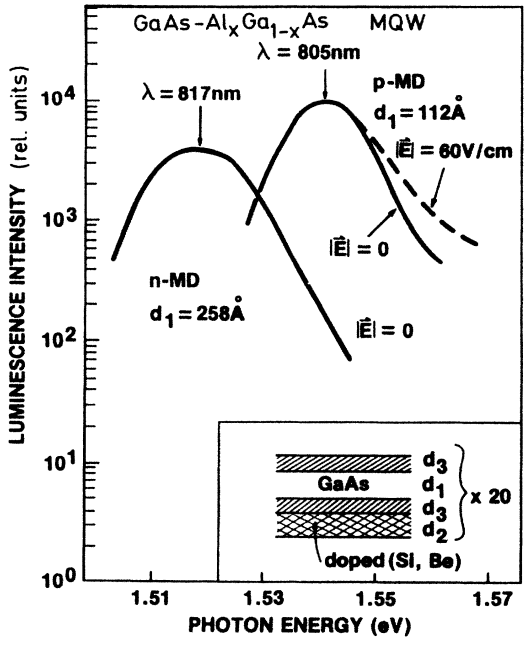


FIG. 3. Luminescence spectra around the band gap of $n$- and $p$-type modulation-doped multiple-quantum-well structures. In the imaging experiments, the monochromator is set to the indicated wavelengths of maximal emission intensities.

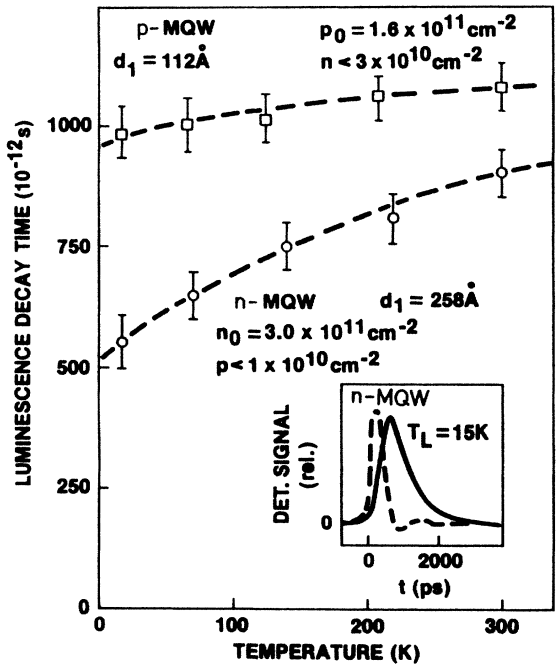


FIG. 4. Luminescence decay times (minority-carrier lifetimes) for the two samples, as a function of temperature. The inset shows the Si-APD response to the 6-ps laser pulse (dashed line) and the time-dependent photoluminescence signal.

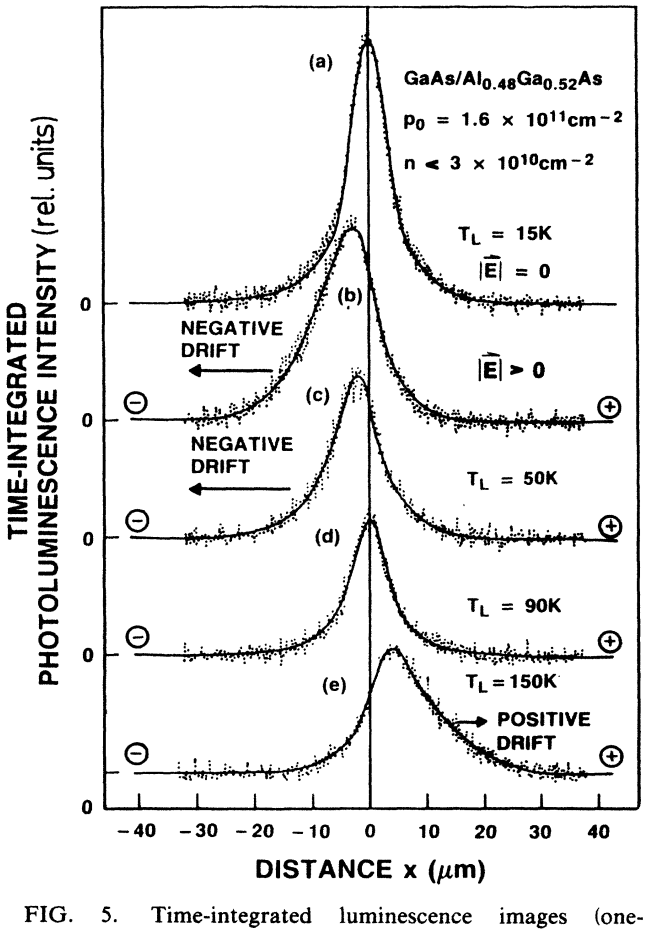


FIG. 5. Time-integrated luminescence images (one-dimensional scans) for different lattice temperatures $T_L = 15$ K, electric field $E = 0$ [curve (a), $E = 20$ V/cm [curve (b)], $T_L = 50$ K, $E = 120$ V/cm [curve (c)], $T_L = 90$ K, $E = 280$ V/cm [curve (d)], and $T_L = 150$ K, $E = 600$ V/cm [curve (e)]. The solid lines are the calculated image shapes according to Eq. (1).

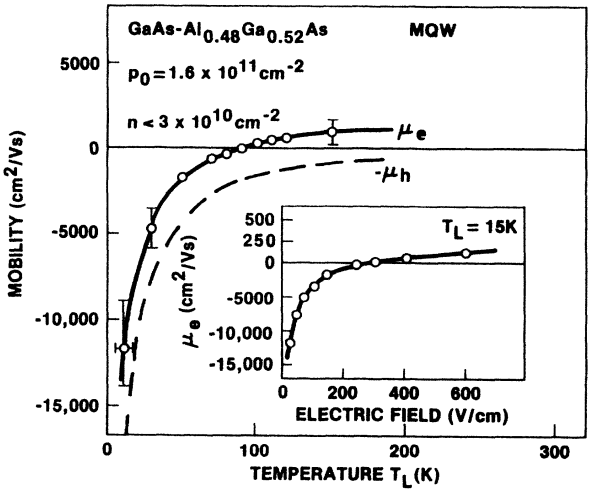


FIG. 6. Minority-electron mobility as a function of the lattice temperature for low electric fields. Circles and solid line: experiment. Dashed line: majority-hole mobility multiplied by $-1$. Inset: electron mobility as a function of electric field at lattice temperature $T_L = 15$ K.

comes zero at $T_L = 90$ K [curve (d)]. Finally, at even higher temperatures [curve (e), $T_L = 150$ K] the drift is in the direction of the positive pole, as expected for negatively charged particles. Curves (b) and (c) demonstrate that, at low temperatures and low electric fields, photoexcited electrons have *negative absolute mobility, i.e., electrons drift towards the negatively charged electrode.*

The experimental data are evaluated by first determining the spatial profile of the photoexcited carriers in the absence of electric fields. In our model (no diffusion), the profile $\int n(x,t)dt$ in the absence of electric fields is identical with the profile $n(x, t = 0)$. An accurate fit can be made with a superposition of two Gaussian (symmetric) curves. The luminescence profiles with applied fields [curves (b)–(e) in Fig. 5] are then fitted by Eq. (1) with the drift velocity $v_d$ as the *only* shape parameter. Equation (1) accurately describes the observed luminescence image: The solid curve and the experimental data, shown in Fig. 5, coincide within the experimental limit of accuracy.

Data from several measurements at different temperatures and different electric fields E are shown in Fig. 6. Here the drift velocities $v_d$, as obtained from the data (similar to those shown in Fig. 5), are expressed by drift mobilities $\mu_e$, according to the definition of electron mobility $\mathbf{v}_d = -\mu_e \mathbf{E}$.[26] The results can be summarized as follows: At low temperatures ($T_L = 15$ K) and low electric fields, the electron-drift mobility is negative. The highest measured value of the negative drift mobility is $-11\,500$ cm$^2$/V s. The negative mobility decreases both with electric field (at 15 K lattice temperature) and with increasing lattice temperature. At temperatures above 90 K the minority-electron mobility becomes positive and increases with increasing temperature. As a function of the electric field (inset, at $T_L = 15$ K), the value of the negative mobility decreases; at higher fields ($> 300$ V/cm) the mobility even becomes positive.

We performed the same experiment with $n$-type modulation-doped quantum-well structures. In this case the spatially and time-resolved luminescence intensity is directly proportional to the local minority-*hole* concentration. Therefore, in this experiment we measure the minority-hole dynamics.[27] All assumptions and experimental details are identical with the $p$-type sample. The $n$-type doped sample has the following parameters: $d_1 = 258$ Å (GaAs), $d_2 = 284$ Å ($Al_{0.23}Ga_{0.77}As$, Si doped), and $d_3 = 118$ Å (undoped $Al_{0.23}Ga_{0.77}As$ "spacer layer" between GaAs and doped $Al_xGa_{1-x}As$). This structure is repeated 15 times on a semi-insulating GaAs substrate. The electron mobilities and concentrations per GaAs layer are $n_0 = 3.0 \times 10^{11}$ cm$^{-2}$ and $\mu_e = 102\,000$ cm$^2$/V s (at 4.2 K), determined by Hall measurements. Concentrations of injected minority holes are below $1 \times 10^{10}$ cm$^{-2}$. The results of the luminescence "imaging" are shown in Fig. 7. The dashed lines are the profiles *without* electric fields and the solid curves are the profiles with applied electric fields.

With applied electric field, at low lattice temperature

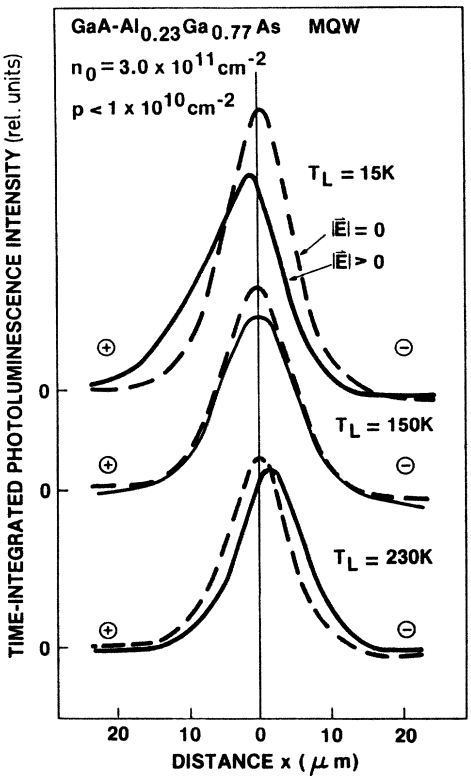


FIG. 7. Time-integrated luminescence images (one-dimensional scans) for different lattice temperatures $T_L$ and electric fields $E$ (solid curves): $T_L=15$ K, $E=13.5$ V/cm (top), $T_L=150$ K, $E=100$ V/cm (middle), and $T_L=230$ K, $E=213$ V/cm (lowest). Dashed curves: $E=0$.

(15 K) the luminescence "image" is shifted towards the positive pole of the applied electric field. This means that injected minority holes in the high-mobility electron plasma also have negative absolute mobility, i.e., the holes drift from the negative to the positive electrode. At a higher lattice temperature ($T_L=150$ K), no drift is measureable, at $T_L=230$ K, the holes drift towards the negative electrode. From the luminescence images we obtain the hole drift velocities and mobilities in the same manner as for the minority electrons. Equation (1), for the holes, can be written as

$$\int I(x,t)dt \propto \int p(x+v_d t, t=0) f_I(t)dt \ . \qquad (2)$$

The time dependence $f_I(t)$, as determined with the Si-APD (avalanche photodiode), follows an exponential decay law with characteristic decay times shown in Fig. 4. The minority-hole lifetimes (luminescence decay times) are shorter than those of minority electrons in the $p$-doped quantum wells, and become somewhat longer at higher temperatures. With known $f_I(t)$ and measured profile $\int I(x,t)dt$, we can again determine $v_d$ as the only shape parameter by fitting the difference of the profiles with electric field and without field. The procedure is the same as described before for the minority electrons (Fig. 5).

Values of the minority-hole mobility, obtained in this manner, are plotted in Fig. 8. The definition of the hole mobility, $v_d=\mu_h E$, was used to obtain the mobility from the drift velocity. As we saw qualitatively already in the "imaging" data (Fig. 7), the hole mobility is negative at low fields and low temperatures. A value of $\mu_h=-40\,000$ cm$^2$/V s is measured at the lowest possible temperature and electric field. The minority-hole mobility becomes positive above lattice temperatures of 150 K. In the same figure the values of the majority-electron mobility—multiplied by $-1$—are plotted, showing a temperature dependence which tends, at least qualitatively, in the same direction. In Sec. IV we will show that majority-electron and minority-hole mobilities are directly related. The inset in Fig. 8 shows the decrease of the negative hole mobility, as higher electric fields are applied.

Summarizing the experimental results, we can say for both minority electrons in a high-mobility hole plasma and minority holes in a high-mobility electron plasma in GaAs quantum wells at low temperatures and low electric fields: The injected minority carriers drift in the *"wrong" electric field direction,* minority electrons towards the negative, minority holes towards the positive electrode. The minority-carrier mobilities, which are therefore negative at low temperatures, become smaller at higher temperatures and finally positive above 150 K. Large electric fields also reduce the negative minority-carrier mobility. We will next explain these surprising effects and their relation to the majority-carrier mobility, on the basis of the strong electron-hole–scattering effects present in these semiconductor structures.

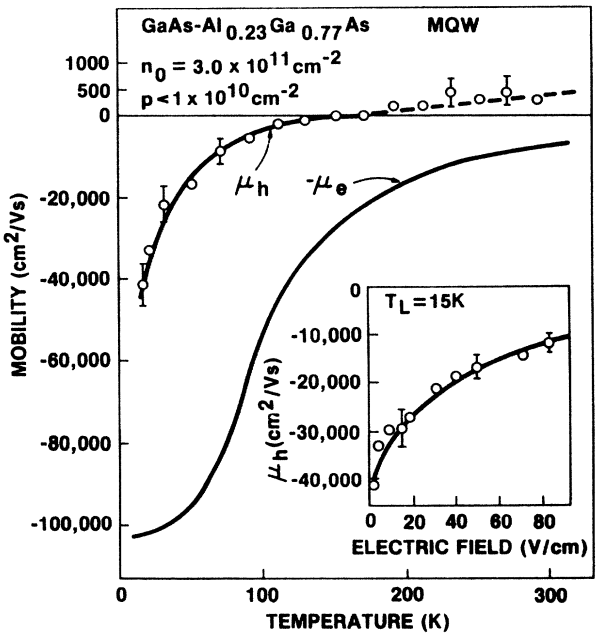


FIG. 8. Minority-hole mobility as a function of the lattice temperature for low electric fields. Circles and solid line: experiment. Lower solid line: majority-electron mobility multiplied by $-1$. Inset: hole mobility vs electric field at lattice temperature $T_L=15$ K.

## IV. ANALYSIS

The dynamics of the minority carriers injected into a high-density majority-carrier plasma are determined by recombination, ambipolar diffusion, and ambipolar mobility.[29] The effects of recombination are considered in the evaluation of the data, using the experimentally determined decay function $f_I(t)$. Diffusion effects can be neglected.[23] The ambipolar mobility is equal to the true minority-carrier mobility, if (for the case of minority electrons) $n\mu_e \ll p\mu_p$.[30] This condition for minority-carrier transport is fulfilled in both experiments ($n$- and $p$-type doped samples). Therefore the space charges of the injected and drifting minority carriers are screened by dielectric relaxation of the majority carrier plasma. The electric field, acting on the minority carriers, is homogeneous and equal to the applied field along the sample. The measured (ambipolar) mobility, once more, is thus the true minority-carrier mobility.

The exact minority-carrier mobility, which *must include the effects of electron-hole scattering,* can be obtained from solving the coupled Boltzmann equations for electrons and holes. Numerical solutions have been obtained by McLean and Paige[4] for the experimental systems of $n$- and $p$-type Ge,[3] as well as for $n$-type InSb. For the analysis of our data we use a hydrodynamic approximation with average relaxation times $\langle\tau\rangle$ that account for the various scattering processes.

If the velocity distributions are drifted Maxwellians with drift velocities $v_e$ and $v_h$, then it can be shown that these equations can be approximated by the coupled hydrodynamic or fluid equations in the relaxation-time approximation:[31]

$$\frac{dv_e}{dt} = -\frac{v_e}{\langle\tau_{e\text{-}L}\rangle} - \frac{v_e - v_h}{\langle\tau_{e\text{-}h}\rangle} - \frac{eE}{m_e} \tag{3}$$

and

$$\frac{dv_h}{dt} = -\frac{v_h}{\langle\tau_{h\text{-}L}\rangle} - \frac{v_h - v_e}{\langle\tau_{h\text{-}e}\rangle} + \frac{eE}{m_h} \,. \tag{4}$$

$\langle\tau_{e\text{-}L}\rangle$ and $\langle\tau_{h\text{-}L}\rangle$ are the momentum relaxation times of electrons and holes (averaged over the energy distribution function) by lattice scattering. $\langle\tau_{e\text{-}h}\rangle$ is the momentum relaxation time of electrons in the *resting* hole plasma by Coulomb scattering, $\langle\tau_{h\text{-}e}\rangle$ is the momentum relaxation time of holes in a *resting* electron plasma. $m_e$ and $m_h$ are the effective electron and hole masses and $E$ is the absolute value of the electric field. The coupled equations (3) and (4) can be solved for the steady state ($dv_e/dt = dv_h/dt = 0$), if we take into account that the total momentum of the plasma is conserved in the process of electron-hole scattering

$$\frac{nm_e}{\langle\tau_{e\text{-}h}\rangle} = \frac{pm_h}{\langle\tau_{h\text{-}e}\rangle} \tag{5}$$

($n$,$p$... total electron and hole sheet concentrations per layer). Then the minority-electron and minority-hole mobilities, as defined earlier, are

$$\mu_e = \frac{e\left[\dfrac{\langle\tau_{e\text{-}h}\rangle}{m_e} + \dfrac{n\langle\tau_{h\text{-}L}\rangle}{pm_h} - \dfrac{\langle\tau_{h\text{-}L}\rangle}{m_h}\right]}{1 + \dfrac{\langle\tau_{e\text{-}h}\rangle}{\langle\tau_{e\text{-}L}\rangle} + \dfrac{nm_e\langle\tau_{h\text{-}L}\rangle}{pm_h\langle\tau_{e\text{-}L}\rangle}} \tag{6}$$

and

$$\mu_h = \frac{e\left[\dfrac{\langle\tau_{h\text{-}e}\rangle}{m_h} + \dfrac{p\langle\tau_{e\text{-}L}\rangle}{nm_e} - \dfrac{\langle\tau_{e\text{-}L}\rangle}{m_e}\right]}{1 + \dfrac{\langle\tau_{h\text{-}e}\rangle}{\langle\tau_{h\text{-}L}\rangle} + \dfrac{pm_h\langle\tau_{e\text{-}L}\rangle}{nm_e\langle\tau_{h\text{-}L}\rangle}} \,. \tag{7}$$

From Eqs. (6) and (7) it becomes clear why it is possible to see *negative* drift or negative absolute mobility of minority carriers. For, e.g., weak minority-electron injection, $n \ll p$, the second term in the numerator can be neglected, and thus $\mu_e$ in Eq. (6) becomes negative, if the minority-carrier mobility *relative* to the majority carrier plasma ($e\langle\tau_{e\text{-}h}\rangle/m_e$) is smaller than the majority-carrier mobility due to lattice scattering ($e\langle\tau_{h\text{-}L}\rangle/m_h$). In other words, *electron-hole scattering, stronger than lattice scattering of majority carriers, causes a "carrier-drag effect" that drags the minority electrons in the same drift direction as the majority-carrier plasma.* The temperature (and electric field) dependence of the minority-carrier mobilities (decrease of the negative mobility and turnover to positive mobility) is qualitatively understandable by the decrease of the majority-carrier mobility with increasing temperature (and electric field), which according to Eqs. (6) and (7) directly affects the magnitude and sign of the minority-carrier mobility.

In our samples, the scattering times of majority electrons and holes by lattice scattering are known from temperature-dependent Hall measurements.[32] The results for the majority-carrier plasmas (in terms of mobilities) are shown in Figs. 6 and 8. The values for the lattice scattering times of the minority carriers are estimated from the data of comparable high-quality samples.[33,34] With all lattice-scattering times known, and the experimental values of the minority-carrier mobilities $\mu_e$ and $\mu_h$, the values of the electron-hole–scattering times $\langle\tau_{e\text{-}h}\rangle$ and $\langle\tau_{h\text{-}e}\rangle$ can be obtained from Eqs. (6) and (7).

Figure 9 shows the results of this analysis. The momentum relaxation times of the minority electrons in the majority-hole plasma, $\langle\tau_{e\text{-}h}\rangle$, and $\langle\tau_{h\text{-}e}\rangle$, the momentum relaxation time of minority holes in the electron plasma, are plotted as a function of temperature. The values of $\langle\tau_{e\text{-}h}\rangle$ are below $10^{-13}$ s ($<100$ fs) for all temperatures, with best values for $\langle\tau_{e\text{-}h}\rangle$ of $80\pm20$ fs around 100 K. The larger error bars at low temperatures are due to the small difference between the (negative) electron mobility and the majority-hole mobility (Fig. 6). At higher temperatures the electron mobility is still considerably below the lattice-scattering-limited mobility: there the determination of $\langle\tau_{e\text{-}h}\rangle$ from Eq. (6) is more accurate.

The values of $\langle\tau_{h\text{-}e}\rangle$ are almost 2 orders of magnitude larger: At low temperatures we obtain $\langle\tau_{h\text{-}e}\rangle = 4\pm1$ ps; at higher temperatures the relaxation time stays in the

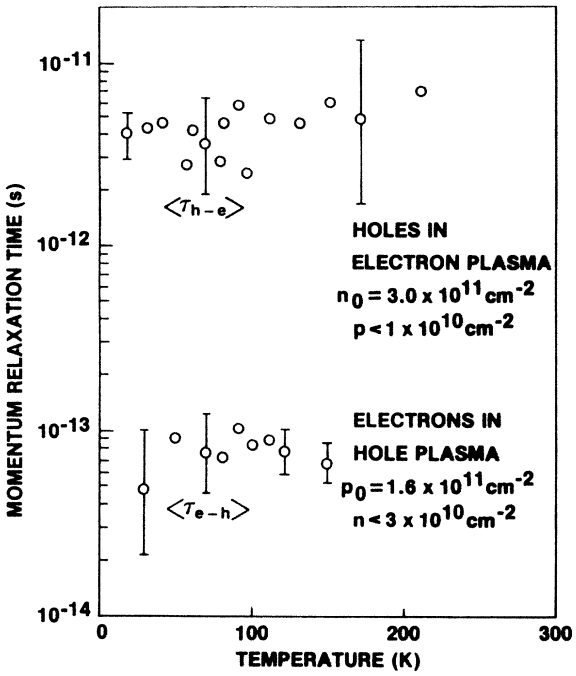


FIG. 9. Momentum relaxation time of minority electrons and minority holes by electron-hole scattering as a function of temperature.

same range. However, the error bars become larger, since the measured hole mobility in the presence of electron-hole scattering comes closer to the lattice-scattering-limited hole mobility in quantum wells. For the whole temperature range we can say that the *momentum relaxation times* $\langle \tau_{e\text{-}h} \rangle$ *and* $\langle \tau_{h\text{-}e} \rangle$ *differ by roughly a factor of 50.* The experimental accuracy sets a lower limit for this factor of at least 30 and an upper limit of about 100, only slightly depending on temperature.

## V. DISCUSSION

The first point of discussion is the question, why does electron-hole scattering cause dramatic transport effects for minority carriers *in quantum wells,* but not in bulk GaAs?[35] The answer is that the strong electron-hole–drag effects observed in our experiments are due to both the *high mobility* of the majority carriers and their *high concentration.* The high concentrations cause short electron-hole–scattering times and the high mobility allows a large effect of a given electron-hole–scattering time on the minority-carrier drift mobility, according to Eqs. (6) and (7). High carrier concentrations *and* high mobilities can be achieved in modulation-doped quantum wells. Therefore, for our experiments quantum wells were the ideal system (in contrast to bulk semiconductors), for a clear observation of electron-hole drag effects, particularly the observed "negative absolute mobility."

We next discuss the measured values of the momentum relaxation times by electron-hole scattering. The values of $\langle \tau_{e\text{-}h} \rangle$, the momentum relaxation time of minority electrons in a hole plasma of $p=1.5$ to $1.9\times10^{11}$ cm$^{-2}$ within a 112-Å quantum-well width, should be comparable to the relaxation times of electrons in highly doped $n$-type GaAs, where ionized-impurity scattering dominates. The hole concentration corresponds to a volume concentration of $(1-2)\times10^{17}$ cm$^{-3}$. At impurity concentrations of these levels, the mobility in $n$-type GaAs is below 5000 cm$^2$/V s—estimated from measurements at lower[36] and higher[37] doping levels, as well as from the mobility values at room temperature.[38] A mobility of less than 5000 cm$^2$/V s corresponds to a momentum relaxation time of less than $1.9\times10^{-13}$ s, which is in fair agreement with our measured electron-hole–scattering times of $80\pm20$ fs around 100 K.

The reverse case, the momentum relaxation of minority holes in an electron plasma, differs in *three* important ways from that of minority electrons in a hole plasma. First, the effective masses of electrons and holes are much different, which directly affects the momentum transfer in the two-component plasma: For an estimate we assume the same relative concentrations for the two cases and the same screening conditions, and $\langle \tau_{e\text{-}h} \rangle$ in first order proportional to $1/p$ (Conwell-Weisskopf formula). Then momentum conservation [Eq. (5)] directly gives

$$\frac{\langle \tau_{h\text{-}e} \rangle}{\langle \tau_{e\text{-}h} \rangle} = \frac{m_h}{m_e} . \tag{8}$$

This means that from classical plasma kinetics we expect $\langle \tau_{e\text{-}h} \rangle$ to be—by a factor of the linear mass ratio—larger than $\langle \tau_{h\text{-}e} \rangle$. Since the majority-electron concentration in our case is even higher than the majority-hole concentration, the ratio should be even smaller; thus $\langle \tau_{h\text{-}e} \rangle / \langle \tau_{e\text{-}h} \rangle$ should be smaller than a value of 6 ($m_e = 0.0665 m_0$, $m_h \approx 0.4 m_0, m_0, \ldots$ free-electron mass), in contrast to the experimental result of about 50.

A second difference is the fact that the majority-electron plasma is degenerate up to temperatures above 100 K, whereas the Fermi energy of the hole plasma, due to the larger effective mass, is much lower. Because there is relatively little energy transfer in the scattering of a heavy hole by a light electron, for $T<100$ K only those electrons near the Fermi energy are permitted, by the exclusion principle, to scatter holes. Hence, in the majority-electron case, degeneracy forces hole-electron collisions to involve electrons of relatively high velocity. Since the Coulomb scattering time varies as (velocity)$^{3/2}$, this effect causes a further enhancement of $\langle \tau_{h\text{-}e} \rangle$ relative to $\langle \tau_{e\text{-}h} \rangle$ for $T<100$ K. As a consequence, we predict a large ratio of relaxation times, $\langle \tau_{h\text{-}e} \rangle / \langle \tau_{e\text{-}h} \rangle$, for low temperature ($T \simeq 20$ K).

Finally, in the experiments reported above, there is an asymmetry in geometry between the $p$- and $n$-type samples that increases $\langle \tau_{h\text{-}e} \rangle$ relative to $\langle \tau_{e\text{-}h} \rangle$ for all temperatures. The carrier concentration in the $n$-type sample is higher ($p_0 = 1.5\times10^{11}$ cm$^{-2}$ versus $n_0 = 3.0\times10^{11}$ cm$^{-2}$), but the $n$-type quantum wells are considerably wider ($d_1 = 258$ Å). The $p$-type quantum wells are thus close to the two-dimensional (2D) limit, whereas the $n$-type sample is more nearly three dimensional (3D); higher subbands are occupied. Also, this should influence the momentum transfer by electron-hole

scattering, due to the different densities of states at low energies and due to the different screening behavior in 2D and 3D systems.

To estimate the effects of different masses and degeneracy, we have calculated the relaxation times, $\langle \tau_{e\text{-}h} \rangle$ and $\langle \tau_{h\text{-}e} \rangle$, assuming drifted Maxwellian and Fermi-Dirac distributions for the carriers. These calculations, which are straightforward but lengthy, are outlined in the Appendix. They confirm the physical picture of the relaxation process outlined above and give fair agreement with the measured relaxation times. In particular, we find

$$\langle \tau_{h\text{-}e} \rangle / \langle \tau_{e\text{-}h} \rangle = \xi (m_h/m_e)(E_F/kT_L)(p/n) , \quad (9)$$

where $E_F$ is the electron Fermi energy (corresponding to $\approx 100$ K), $T_L$ the sample temperature, and $\xi$ a numerical factor that depends on the sample geometries (2D versus 3D). For our case, in which the $n$-type sample is more three dimensional than the $p$-type sample, $\xi \simeq 6$.

At $T_L = 100$ K, where the measurements of $\langle \tau_{e\text{-}h} \rangle$ and $\langle \tau_{h\text{-}e} \rangle$ are relatively accurate, we calculate $\langle \tau_{e\text{-}h} \rangle = 60$ fs compared to the experimental value $\langle \tau_{e\text{-}h} \rangle = 80$ fs, and $\langle \tau_{h\text{-}e} \rangle = 1.5$ ps compared to the experimental value $\langle \tau_{h\text{-}e} \rangle = 4$ ps. The agreement is surprisingly good considering the approximations made in computing $\langle \tau_{e\text{-}h} \rangle$ and $\langle \tau_{h\text{-}e} \rangle$.

It would also be interesting to confirm the prediction that $\langle \tau_{e\text{-}h} \rangle$ becomes exceedingly small at low temperatures (the calculations imply $\langle \tau_{e\text{-}h} \rangle \simeq 12$ fs at 20 K). Unfortunately, in this temperature range, $\langle \tau_{e\text{-}h} \rangle$ is determined from the small difference of two relatively large numbers ($\mu_p - |\mu_e|$), which precludes an experimental test of this implication of the theory. In addition, an exact calculation and comparison of the two cases is very complex and would require the exact theories of screening and the influences of the higher subbands and intersubband transitions.

At this point we want to mention a further quantitative result on the momentum relaxation time by electron-hole scattering: From time-of-flight measurements of the minority-electron velocity in $p$-type doped quantum wells at room temperature[17,19] we obtained a low-field mobility of the minority electrons, which was much smaller (around 1500 $cm^2/V\,s$) than the known room-temperature electron mobility in high-purity GaAs (around 8000 $cm^2/V\,s$). These measurements are described in detail in Refs. 17 and 19, and also discussed in Sec. VII of the present paper. From the low value of mobility we obtain (using a lattice-scattering mobility of 8000 $cm^2/V\,s$) a momentum relaxation time of $\approx 70$ fs, which is very close to the data discussed above. We interpret this by the different hole concentrations in the two samples: The higher temperature would increase the relaxation time, the higher hole concentration in the time-of-flight measurements at room temperature ($4.2 \times 10^{11}$ $cm^{-2}$) makes the momentum scattering more effective. This explains roughly the similar order of magnitude of the relaxation time in these two very different regimes.

## VI. PHOTOCONDUCTIVITY

A further point of discussion is photoconductivity in the range of "negative absolute mobility": As will be shown in the following, the photoconductivity signal should be negative in this range; the extreme electron-hole drag should *reduce* the conductivity of the sample. The criterion for negative absolute mobility coincides exactly with the occurrence of negative photoconductivity. In the following this is proven for the case of an $n$-type modulation-doped quantum well with injected minority holes. The change of the sheet conductivity $\Delta\sigma$ by injecting minority carriers (concentration $p$) into the majority-carrier plasma of concentration $n_0$ ($p_0 = 0$) is given as

$$\Delta\sigma = ne\mu_e + pe\mu_p - n_0 e\mu_{e\text{-}L} , \quad (10)$$

with $\mu_{e\text{-}L}$ the majority-electron mobility without the presence of holes (only lattice scattering). Substituting Eqs. (6) and (7) for $\mu_e$ and $\mu_p$ gives the exact result for $\Delta\sigma$. Setting $\mu_p = 0$ in Eq. (10),

$$\Delta\sigma = \frac{ne^2 \left[ -\dfrac{\langle \tau_{e\text{-}L} \rangle}{m_e} + \dfrac{p \langle \tau_{e\text{-}L} \rangle}{nm_e} + \dfrac{\langle \tau_{h\text{-}e} \rangle}{m_h} \right]}{1 + \dfrac{\langle \tau_{e\text{-}h} \rangle}{\langle \tau_{e\text{-}L} \rangle} + \dfrac{nm_e \langle \tau_{h\text{-}L} \rangle}{pm_h \langle \tau_{e\text{-}L} \rangle}} . \quad (11)$$

The numerator is identical with the numerator of Eq. (7) for $\mu_h$ (times $ne$), so that $\mu_h = 0$ implies $\Delta\sigma = 0$. The photoconductivity thus goes from positive through zero exactly when the mobility becomes negative. This condition is valid independent of the lattice-scattering parameters.

A negative photoconductivity signal with the same decay time as the photoluminescence, however, could *not* be observed in our samples. The $p$-type doped samples reveal high negative photoconductivity with a decay time of $\approx 2.5$ ms (at 15 K), as well as a small positive photoconductivity signal with a decay time of $\approx 20$ ns. Both effects clearly are not related to the minority-carrier dynamics in GaAs, where the luminescence decays with a lifetime of 1 ns. The effects are probably related to trapping of carriers in $Al_xGa_{1-x}As$, as reported in Ref. 20, as well as to parallel conductivity in $Al_xGa_{1-x}As$, since we excite carriers in both GaAs and $Al_xGa_{1-x}As$. The $n$-type samples also show photoconductivity signals of much longer decay times than the photoluminescence. Also in the $n$-type samples, carriers are injected in both GaAs and $Al_xGa_{1-x}As$, and, therefore, the parallel photoconductivity in $Al_xGa_{1-x}As$ probably masks the negative photoconductivity signal from the negative drift of the minority carriers in GaAs. Recently, spectrally resolved photoconductivity measurements were performed in these samples,[39] which showed negative photoconductivity below the band gap of GaAs. This effect, however, was shown to be of different origin, and not correlated to the negative mobility.

## VII. ENERGY TRANSFER

In a different set of experiments we measured the minority-electron energy distribution at high electric

fields in the presence of electron-hole scattering. The results of these experiments are relevant for this paper, since from these experiments the *energy-transfer rate* between electrons and holes can be determined and, subsequently, the energy relaxation times of hot electrons in a cold hole plasma by electron-hole scattering. The experiments were originally reported in Ref. 17, and are reviewed here and quantitatively analyzed.

The experments were performed by injection of minority electrons in $p$-type modulation-doped quantum wells (similar to the $p$-type samples used in the "carrier-drag" experiment) by use of picosecond photoexcitation. By measuring simultaneously (1) the electron velocity by a time-of-flight technique, (2) the luminescence spectra, and (3) the hole current as a function of the applied electric field, we were able to determine quantitatively the energy distribution of the electrons (electron temperature), the hole temperature, and the total energy-loss rate of minority electrons in a hole plasma. The most striking result was the observation of a nonequilibrium plasma state with different distribution functions for electrons and holes. The distribution functions of minority electrons at high fields are found to be "hot" distributions, in contrast to the hole plasma, which remains close to room temperature.

The total energy-loss rate per electron is much larger (by about a factor of 2) in the presence of a hole plasma than in the absence of holes. The difference of the two rates is attributed to energy loss by electron-hole scattering, which provides net energy transfer from electrons to holes in the nonequilibrium state.

In Fig. 10 the main results of the experiments are shown. The measured minority-electron temperature (from the exponential slope of the luminescence spectra) is plotted versus the energy-loss rate per electron. The energy-loss rate per electron, $\langle d\epsilon/dt \rangle_{\text{total}}$, in the steady state must be equal to the input power per electron, $e\mu_e E^2$. The minority-electron mobility $\mu_e$, in the applied electric field $E$, is directly measured by a time-of-flight technique ($e$. . . electron charge). Figure 10 shows that the measured total energy-loss rate (experimental data, solid curve and circles) is much larger than the calculated energy-loss rate of majority electrons by (optical-) phonon emission. The dashed curve is the energy-loss rate $\langle d\epsilon/dt \rangle_{e\text{-ph}}$ of majority electrons in identical quantum wells, when no electron-hole scattering is present. The values are obtained by using the experimental results for the electron-phonon coupling,[40] and the theoretical temperature dependence[41] for the high-temperature range. Since the total energy loss is the sum of the energy-loss rates due to phonon emission and due to electron-hole scattering,

$$\langle d\epsilon/dt \rangle_{\text{tot}} = \langle d\epsilon/dt \rangle_{e\text{-ph}} + \langle d\epsilon/dt \rangle_{e\text{-}h} , \tag{12}$$

we can determine $\langle d\epsilon/dt \rangle_{e\text{-}h}$ as the difference between the measured total energy-loss rate and the energy-loss rate by phonon emission. The result is shown in Fig. 10 as the dotted curve $\langle d\epsilon/dt \rangle_{e\text{-}h}$. The energy-loss rate increases with increasing electron temperature, and agrees roughly with the theoretical curve $\langle d\epsilon/dt \rangle_{e\text{-}h}$(theor).

For this theoretical estimate, we used a solution of the Fokker-Planck equation, which has been derived for the analogous problem in a gas plasma, the energy transfer between electrons and ions by Coulomb collisions.[42,43] The equations and parameters used are contained in Ref. 17.

With the definition for an energy relaxation time of electrons in a two-dimensional hole plasma of temperature $T_h$,

$$\langle d\epsilon/dt \rangle_{e\text{-}h} = -\frac{k_B(T_e - T_h)}{\langle \tau_\epsilon \rangle_{e\text{-}h}} , \tag{13}$$

we can give quantitative values of the energy relaxation time $\langle \tau_e \rangle_{e\text{-}h}$ by electron-hole scattering. In Fig. 11 the so-obtained energy relaxation times are shown as a function of electron temperature. The total experimentally measured energy relaxation time is around 200 fs, increasing with temperature. Electron-hole scattering and electron-phonon emission show energy relaxation times between 200 and 500 fs.

These values are the first reported data on the energy-transfer times between electrons and holes in semiconductors. The energy relaxation times are in reasonable agreement with our results of momentum relaxation times: We expect for the energy relaxation *longer* characteristic times than for the momentum relaxation, due to the large difference of electron and hole masses. An exact quantitative comparison is difficult, since the hole concentration in the energy relaxation experiment (Fig. 11) is higher than in the electron-hole drag experiment, and both carrier and lattice temperatures are in different ranges. Finally, we want to point out that both energy relaxation times, $\langle \tau_\epsilon \rangle_{e\text{-}h}$ and $\langle \tau_\epsilon \rangle_{e\text{-ph}}$ are *increasing* with temperature. For electron-hole scattering this is obvious from the energy dependence of Coulomb scattering (decreasing scattering cross section with increasing particle velocity[43]). For electron-phonon scattering the physical

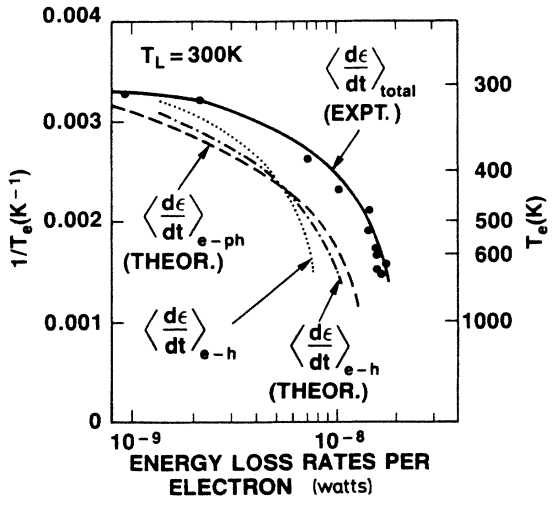


FIG. 10. Electron temperatures vs energy-loss rate for the different scattering mechanisms (electron-phonon scattering, electron-hole scattering) and experimental results (circles and solid line).

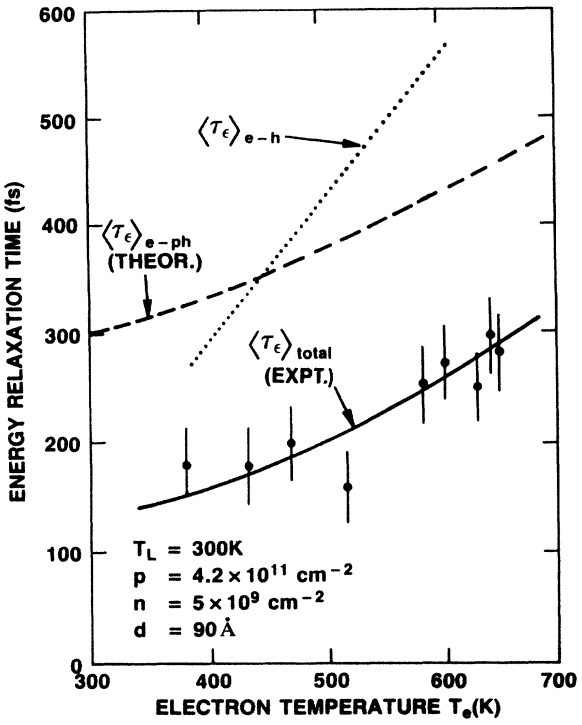


FIG. 11. Energy relaxation times of minority electrons as a function of electron temperature, by electron-hole scattering (dotted line), phonon emission (dashed), and the total energy relaxation time (solid lines and circles).

reason is the onset of the "polar runaway effect,"[41] which leads to a finite energy loss for $T_e \rightarrow \infty$ and, therefore, to a diverging energy relaxation time at high electric fields.

## VIII. SUMMARY

In modulation-doped quantum wells with high majority-carrier densities and high mobilities, the transport of minority carriers is strongly influenced by electron-hole scattering. At low temperatures the momentum transfer from majority to minority carriers is large enough to cause carrier drag, with drift velocities of the minority carriers in the *same* direction as the majority-carrier drift. This *"negative drift"* or *"negative absolute mobility"* is experimentally shown directly by the spatially and time-resolved photoluminescence: minority electrons drift towards the negative electrode, minority holes towards the positive.

From the measured minority- and majority-carrier mobilities, applying a hydrodynamic model in the relaxation-time approximation, we obtain quantitative values of the electron-hole momentum relaxation times. The electron-hole momentum relaxation time of minority electrons in *p*-type doped quantum wells is extremely short (50–100 fs), but is expected from a comparison with ionized-impurity scattering in highly doped *n*-type GaAs. The momentum relaxation time of holes in a high-density electron plasma of *n*-type modulation-doped quantum wells is longer by almost 2 orders of magnitude (2–5 ps). A factor of the linear mass ratio (about 6) is expected from the classical mechanics of the momentum transfer by Coulomb collisions. We attribute the remaining difference to two effects: The more two-dimensional character of the *p*-type sample enhances the momentum scattering rate as compared to the more three-dimensional *n*-type plasma. Second, the degeneracy of the majority-electron plasma reduces by phase-space filling the momentum transfer of electron-hole scattering. In a different set of experiments we measured the energy relaxation of hot electrons (electron temperature far above room temperature) by electron-hole scattering (hole temperature close to room temperature). Energy relaxation times by electron-hole scattering range from 200 fs ($T_e = 300$ K) to 500 fs ($T_e > 600$ K).

There are several open areas of further theoretical and experimental work related to this work: the expected negative photoconductivity in the state of negative mobility has not been experimentally verified yet. Theories of electron-hole scattering including screening and the influences of the quantum confinement (subbands, two-dimensional plasma properties, etc.) would be of high interest. At this point we want to refer to recent theoretical works on electron-hole scattering, by analytical theories[44] as well as ensemble Monte Carlo calculations.[45] Furthermore, the strong field dependence of the negative absolute mobility (Fig. 6, inset) might have implications for questions of instabilities in such two-component plasmas. Finally, it would be interesting to find other experimental systems, where "negative absolute mobility" due to electron-hole scattering can be observed and studied.

## ACKNOWLEDGMENTS

We gratefully acknowledge collaboration with A. E. Di Giovanni, T. C. Damen, D. Block, and W. Wiegmann. K. Baldwin performed the Hall measurements. We thank A. Pinczuk, H. L. Störmer, and G. E. Stillmann for valuable discussions, and W. Seidenbusch for a critical reading of the manuscript. One of us (R.A.H.) likes to acknowledge support by the Fonds zur Förderung der wissenschaftlichen Forschung (Vienna, Austria), under Project No. P-6184, and also AT&T Bell Laboratories (Holmdel, NJ), where the experimental work was performed.

## APPENDIX

In a two-dimensional *p*-type quantum well the rate of change of the injected electron momentum distribution, due to electron-hole collisions, is given by the expression

$$\left.\frac{\partial f(p)}{\partial t}\right|_{e\text{-}h} = -\left[\frac{2\pi}{\hbar}\right]\int\int\left[\frac{f(p)\,|\,V(q_\perp)\,|^2}{\mathcal{A}^2}N_P F(P)\delta\left[\frac{p^2}{2m^*}+\frac{P^2}{2M^*}-\frac{(p+\hbar q_\perp)^2}{2m^*}-\frac{(P-\hbar q_\perp)^2}{2M^*}\right]\right]\frac{\mathcal{A}}{(2\pi)^2}d^2q_\perp d^2P$$
$$+\left[\frac{2\pi}{\hbar}\right]\int\int\left[\frac{f(p+\hbar q_\perp)\,|\,V(q_\perp)\,|^2}{\mathcal{A}^2}N_P F(P-\hbar q_\perp)\right.$$
$$\left.\times\delta\left[\frac{p^2}{2m^*}+\frac{P^2}{2M^*}-\frac{(p+\hbar q_\perp)^2}{2m^*}-\frac{(P-\hbar q_\perp)^2}{2M^*}\right]\right]\frac{\mathcal{A}}{(2\pi)^2}d^2q_\perp d^2P\ . \tag{A1}$$

Here $f(p)$ is the two-dimensional momentum distribution describing electron motion in the plane of the quantum well, $F(P)$ is the corresponding quantity for holes, and $\mathcal{A}$ is the area. The Coulomb interaction between electrons and holes is treated in Born approximation. We will generally assume that only a single subband is occupied in both the conduction and valence bands. $V(q_\perp)$ then takes the form

$$V(q_\perp)=\int\int\int\left[\frac{4\pi e^2}{\epsilon_0(q_\perp^2+q_z^2)}e^{iq_z(z-z')}\,|\,\phi_e(z)\,|^2\,|\,\phi_p(z')\,|^2\right]\frac{1}{2\pi}dz\,dz'dq_z\ , \tag{A2}$$

where $\phi_e(z)$ is the wave function of the lowest electron subband and $\phi_p(z)$ that of the topmost hole subband. To evaluate Eq. (A1), we make the drastic assumption that $f(p)$ and $F(P)$ are *drifted Maxwellian* distributions. In the majority-hole case this assumption has some validity for $T\gtrsim 20$ K, at which point the hole distribution becomes degenerate. It should be clearly understood, however, that the drifted Maxwellian approximation can cause sizable errors in transport coefficients—a factor of 2 in one case discussed by McLean and Paige.[4] We suspect that the errors are smaller in the example treated here, but nevertheless do not claim accuracy greater than a factor of 2 for the momentum relaxation rate caused by electron-hole scattering. Though crude, the drifted Maxwellian approximation has the great advantage of permitting an almost exact evaluation of the integrals appearing in Eq. (A1).

After transforming to the rest frames of the two distributions and averaging over electron momenta, one obtains the following formula for the rate of change of the average electron momentum:

$$\left.\frac{d\langle p\rangle}{dt}\right|_{e\text{-}h}=\left[\frac{2\pi}{\hbar}\right]\int\int\int\left[(\hbar q_\perp)f(p)\,|\,V(q_\perp)\,|^2N_P F(P)\right.$$
$$\left.\times\delta\left[\frac{p^2}{2m^*}+\frac{P^2}{2M^*}-\frac{(p+\hbar q_\perp)^2}{2m^*}-\frac{(P-\hbar q_\perp)^2}{2M^*}-(\hbar q_\perp\Delta v)\right]\right]\frac{1}{(2\pi)^2}d^2q_\perp d^2p\,d^2P\ , \tag{A3}$$

where $N_P$ is the hole density per cm$^2$, $f(p)$ and $F(P)$ are Maxwellian distributions, and $\Delta v\equiv v-V$ is the drift velocity of the electrons relative to the holes. Equation (A3) is our basic formula that will be used to calculate the electron-hole relaxation rate.

To evaluate $V(q_\perp)$ from Eq. (A2), we assume that the quantum wells have rectangular potentials with high barriers. The wave functions then are

$$\phi_e(z)\simeq\phi_p(z)\simeq\left[\frac{2}{d}\right]^{1/2}\cos\left[\frac{\pi z}{d}\right]\ , \tag{A4}$$

where $d$ is the width of the quantum well. This approximation is fairly accurate in the minority-electron case; however, there is considerable band bending in the wider, more heavily doped $n$-type quantum wells. Note that the Coulomb interaction is *unscreened* in Eq. (A2); screening is known to be less effective in 2D carrier systems.

The $z$ and $z'$ integrations in Eq. (A2) can be evaluated with the wave functions of Eq. (A4); one finds

$$V_{(q_\perp)}=\int_{-\infty}^{\infty}dq_z\frac{1}{2\pi}\frac{4\pi e^2}{\epsilon_0(q_z^2+q_\perp^2)}\frac{4\kappa^4}{d^2q_z^2(\kappa^2-q_j^2)^2}\sin^2\left[\frac{q_z d}{2}\right]$$
$$=\left[\frac{4\pi e^2}{\epsilon_0 d^2 q_\perp^3}\right]\left[\frac{\kappa^4}{(q_\perp^2+\kappa^2)^2}(e^{-q_\perp d}-1)+dq_\perp+\frac{dq_\perp^3}{2(\kappa^2+q_\perp^2)}\right]\ , \tag{A5}$$

where $\kappa\equiv 2\pi/d$. Note that in the limit of small $q_\perp$, $V(q_\perp)$ is approximately $2\pi e^2/\epsilon_0 q_\perp$; this is a well-known result for the 2D electron gas.

With Maxwellian distributions, the integrals over components of $p$ and $P$ normal to $q_\perp$ in Eq. (A3) can be evaluated immediately, since these variables do not appear in the $\delta$ function. The result is

$$\left.\frac{d\langle p\rangle}{dt}\right|_{e\text{-}h}=\left[\frac{2\pi N_P}{\hbar}\right]\int\cdots\int\left[(\hbar q_\perp)\,|\,V(q_\perp)\,|^2\frac{e^{-p^2/2m^*kT}}{(2\pi m^*kT)^{1/2}}\frac{e^{-P^2/2M^*kT}}{(2\pi M^*kT)^{1/2}}\right.$$
$$\left.\times\delta\left[\frac{\hbar q_\perp P}{M^*}-\frac{\hbar q_\perp p}{m^*}-\frac{(\hbar q_\perp)^2}{2m^*}-\frac{(\hbar q_\perp)^2}{2M^*}-\hbar(q_\perp\Delta v)\right]\right]\frac{1}{(2\pi)^2}dp\,dP\,d^2q\ . \tag{A6}$$

For small $\Delta v$, the integrals over $dp$ and $dP$ appearing here can be evaluated in straightforward way. After some algebra, one finds

$$\left.\frac{d\langle v_e\rangle}{dt}\right|_{e\text{-}h}=\frac{1}{m^*}\left.\frac{d\langle p\rangle}{dt}\right|_{e\text{-}h}=\left[\frac{2\pi N_P}{\hbar}\right]\int\int d^2q_\perp\frac{1}{(2\pi)^2}\left\{|\,V(q_\perp)\,|^2\frac{\hbar(q_\perp\Delta v)}{(1+m^*/M^*)^{1/2}}\left[\frac{1}{2\pi m^*kT}\right]^{1/2}\left[\frac{1}{2kT}\right]\right.$$
$$\left.\times\left[\exp\left[\frac{(\hbar q_\perp)^2}{8m^*kT}\right]\left[\frac{1+m^*}{M^*}\right]\right]\right\}$$
$$=\left[\frac{N_P}{2h}\right]\int_0^\infty dq_\perp\hbar q_\perp^2\left\{|\,V(q_\perp)\,|^2\frac{\Delta v}{(1+m^*/M^*)^{1/2}}\left[\frac{1}{2\pi m^*kT}\right]^{1/2}\left[\frac{1}{2kT}\right]\right.$$
$$\left.\times\exp\left[-(\hbar q_\perp)^2\left[1+\frac{m^*}{M^*}\right]\right]\Big/8m^*kT\right\}\ . \tag{A7}$$

With $|\,V(q_\perp)\,|^2$ replaced by its small-$q_\perp$ limit, $2\pi e^2/\epsilon_0 q_\perp$, this integral has the value

$$\frac{d\langle v_e\rangle}{dt}\simeq\frac{N_P}{16\hbar kT}\left[\frac{4\pi e^2}{\epsilon_0}\right]^2\Delta v\ . \tag{A8}$$

A more accurate result is obtained from a power series expansion of $|\,V(q_\perp)\,|^2$. At 100 K we find, for the $p$-type sample discussed above,

$$\frac{d\langle v_e\rangle}{dt}\simeq(1.6\times10^{13})\Delta v\ \mathrm{s}^{-1}\ .$$

The corresponding electron-hole relaxation is 60 fs, in good agreement with the experimental value of 80 fs at 100 K.

Note that according to Eq. (A8), $\langle 1/\tau_{e\text{-}h}\rangle$ scales as $(kT)^{-1}$. Thus, exceedingly small relaxation times, $\langle\tau_{e\text{-}h}\rangle\simeq15$–$20$ fs, are predicted at 20 K. The Born approximation probably fails in this range. It is even conceivable that the cold electrons localize in the random, drifting potential of the holes.

### 1. Case of minority holes in 2D

We next consider the case of minority holes drifting through a 2D electron gas. For the $n$-type sample, the electrons remain degenerate to about 100 K. Thus, the analysis must be modified to include the effect of the exclusion principle on electron-hole scatterings. The formula analogous to Eq. (A6) is then

$$\left.\frac{d\langle P\rangle}{dt}\right|_{h\text{-}e}=-\left[\frac{2\pi}{\hbar}\right]\int\cdots\int\left[(\hbar q_\perp)F(P)\,|\,V(q_\perp)\,|^2f(p)[1-f(p+\hbar q_\perp)]\right.$$
$$\left.\times\delta\left[\frac{p^2}{2m^*}-\frac{Pq_\perp}{M^*}-\frac{(p+\hbar q_\perp)^2}{2m^*}-\frac{(\hbar q_\perp)^2}{2M^*}-\hbar(q\,\Delta v)\right]\right]\frac{1}{(2\pi)^4\hbar^2}dP\,d^2p\,d^2q_\perp\ . \tag{A9}$$

This integral is considerably more complicated than that of Eq. (A6); to simplify it we make the further approximations $m^*/M^*\to0$ and $kT_{\mathrm{elects}}\simeq0$ (extreme degeneracy). The integral over hole momenta ($P$) can then be performed, and the electron Fermi functions become step functions. Hence

$$\left.\frac{d\langle P\rangle}{dt}\right|_{h\text{-}e}=-\left[\frac{2\pi}{\hbar}\right]\int\cdots\int\left[(\hbar q_\perp)\,|\,V(q_\perp)\,|^2\Theta\left[E_F-\frac{p^2}{2m^*}\right]\Theta\left[\frac{(p+\hbar q_\perp)^2}{2m^*}-E_F\right]\right.$$
$$\left.\times\delta\left[\frac{p^2}{2m^*}-\frac{(p+hq_\perp)^2}{2m^*}-\hbar(q\,\Delta v)\right]\right]\frac{1}{(2\pi)^4\hbar^2}d^2p\,d^2q_\perp\ . \tag{A10}$$

With the changes of variables $x = p^2/2m^*$ and $y = (p + \hbar q_\perp)^2/2m^*$, we find

$$\left.\frac{d\langle P\rangle}{dt}\right|_{h\text{-}e} \simeq + \left[\frac{2\pi}{\hbar}\right]\frac{(2m^*)^2}{(2\pi)^4\hbar^2}\int\cdots\int\left[(\hbar q_\perp)\,|\,V(q_\perp)\,|^2\frac{\Theta(E_F - x)\Theta(x - E_F - \hbar(q_\perp \Delta v))}{[4\hbar^2k_F^2\hbar^2q_\perp^2 - (\hbar q_\perp)^4]^{1/2}}\right]dx\,d^2q_\perp\,, \tag{A11}$$

where the integral goes over values of $q_\perp$ that make the square root real. After some algebra this expression can be rewritten in the form, valid for small $\Delta v$,

$$\left.\frac{d\langle P\rangle}{dt}\right|_{h\text{-}e} \simeq \frac{(m^*)^2}{\pi^3\hbar^3}\int_0^{2k_F}\frac{q_\perp^2\,|\,V(q_\perp)\,|^2}{(4k_F^2 - q_\perp^2)^{1/2}}dq_\perp\,, \tag{A12}$$

where $k_F$ is the Fermi wave vector.

In the 2D limit ($2k_Fd < 1$), the corresponding momentum relaxation time is

$$\left[\frac{1}{\langle\tau_{h\text{-}e}\rangle}\right] = \frac{n_e}{8\pi\hbar E_F}\left[\frac{4\pi e^2}{\epsilon_0}\right]^2\left[\frac{m^*}{M^*}\right]. \tag{A13}$$

This expression should be compared to Eq. (A8). It is smaller by the factor $(2m^*/\pi M^*)$, and contains $E_F$ in place of $kT$. Thus, in the 2D limit

$$\left[\frac{\langle\tau_{h\text{-}e}\rangle}{\langle\tau_{e\text{-}h}\rangle}\right] \simeq \left[\frac{\pi M^*}{2m^*}\right]\left[\frac{E_F}{kT}\right]\left[\frac{N_P}{n_e}\right]. \tag{A14}$$

For our samples, this ratio has the value 7 for $T = 100$ K, which is well below the measured value of 50–60. The corresponding scattering time is $\langle\tau_{h\text{-}e}\rangle \simeq 0.2\times10^{-12}$ s—again far too small. However, the $n$-type sample is actually quite far from the 2D limit ($2k_Fd \simeq 7$). Numerical evaluation of Eq. (A12) shows that, as the quantum wells become more nearly three dimensional, the hole-electron time increases (because of the more rapid cutoff of the $q_\perp$ integration in the 3D limit). We calculate $\langle\tau_{h\text{-}e}\rangle \simeq 1.5\times10^{-12}$ s for the $n$-type sample, a factor of 3 below experiment. Inclusion of screening, which becomes important in the 3D case, will further increase $\tau_{h\text{-}e}$.

Finally, we note from Eq. (A8) that $\langle\tau_{e\text{-}h}\rangle$ becomes exceedingly short at low temperatures ($\langle\tau_{e\text{-}h}\rangle \simeq 12\times10^{-15}$ s at 20 K), whereas $\langle\tau_{h\text{-}e}\rangle$ is temperature independent below $T \simeq 100$ K. From the experimental data it is not possible to test this prediction, although the data do suggest some decrease in $\langle\tau_{e\text{-}h}\rangle$.


[1] J. R. Haynes and W. Shockley, Phys. Rev. **75**, 691 (1949); **81**, 835 (1951).

[2] A. Neukermans and G. S. Kino, Phys Rev. B **7**, 2693 (1973), and references therein.

[3] E. G. S. Paige, J. Phys. Chem. Solids **16**, 207 (1960).

[4] T. P. McLean and E. G. S. Paige, J. Phys. Chem. Solids **16**, 220 (1960).

[5] J. Krausse, Solid State Electron. **15**, 1377 (1972).

[6] F. Dannhauser, Solid State Electron. **15**, 1371 (1972).

[7] G. N. Galkin, E. V. Satkovskii, Litov. Fiz. Sb **16**, 117 (1976) [Sov. Phys.—Collect. **16**, 70 (1976)].

[8] J. R. Meyer and M. Glicksman, Phys. Rev. B **17**, 3227 (1978).

[9] F. J. Bartoli, R. E. Allen, L. Esterowitz, and M. R. Kruer, Solid State Commun. **25**, 963 (1978).

[10] I. V. Kukushkin, Zh. Eksp. Teor. Fiz. **86**, 318 (1984) [Sov. Phys.—JETP **59**, 183 (1984).

[11] M. Morohashi, N. Sawaki, and I. Akasaki, Japan J. Appl. Phys. **24**, 732 (1985).

[12] Instead of the term "carrier drag," the expression "current drag" is used in W. Hansch and G. D. Mahan, J. Phys. Chem. Solids **44**, 663 (1983).

[13] We use the term "negative *absolute* mobility" in order to clearly differentiate true negative mobility from negative *differential* mobility—a completely different phenomenon, for which the term negative mobility is sometimes (wrongly) used.

[14] A transient negative mobility effect in a gas plasma has recently been observed by J. M. Warman, U. Sowada, and Matthijs P. De Haas, Phys. Rev. A **31**, 1974 (1985).

[15] R. A. Höpfel, J. Shah, P. A. Wolff, and A. C. Gossard, Phys. Rev. Lett. **56**, 2736 (1986).

[16] R. A. Höpfel, J. Shah, P. A. Wolff, and A. C. Gossard, Appl. Phys. Lett. **49**, 572 (1986).

[17] R. A. Höpfel, J. Shah, and A. C. Gossard, Phys. Rev. Lett. **56**, 765 (1986).

[18] The minimum resolvable drift length is of the order of 1 $\mu$m; therefore, with lifetimes $\tau_{rec}$ of $\simeq 1$ ns, drift velocities as low as $1\times10^5$ cm/s can be measured.

[19] R. A. Höpfel, J. Shah, D. Block, and A. C. Gossard, Appl. Phys. Lett. **48**, 148 (1986).

[20] M. J. Chou, D. S. Tsui, and G. Weimann, Appl. Phys. Lett. **47**, 609 (1985).

[21] For example, see K. Seeger, *Semiconductor Physics,* 2nd ed. (Springer-Verlag, Berlin, 1982), Chap. 13.

[22] This was verified experimentally by varying the injection density over a large range. The profile of the drifting carriers was unaffected, so it can be assumed that, in the experimental range, the drift velocity is independent of the local carrier concentration and thus homogeneous along the "packet."

[23] Diffusion can be neglected since the diffusion lengths are small compared to the size of the excitation spot.

[24] Since the time dependence of the luminescence follows an exponential behavior with *one* characteristic recombination time, $f_I(t)$ can be assumed independent of the minority-carrier concentration and therefore homogeneous along the carrier packet.

[25] For a review on modulation-doped quantum-well structures, see A. C. Gossard and A. Pinczuk, in *Synthetic Modulated Structures,* edited by L. L. Chang and B. C. Giessen (Academic, New York, 1985), p. 215.

[26] R. A. Smith, *Semiconductors* (Cambridge University Press, Cambridge, 1964), p. 96.

[27]First results on such experiments in a different sample have been published in Ref. 17; in the present work we use a better sample with higher mobility and no "extrinsic" effects (Ref. 28).

[28]J. Shah, A. Pinczuk, H. L. Störmer, A. C. Gossard, and W. Wiegmann, Appl. Phys. Lett. **42**, 55 (1983).

[29]W. van Roosbroek, Phys. Rev. **91**, 282 (1953).

[30]*Semiconductor Physics,* Ref. 21, Chap. 5.

[31]E. P. Gross and E. A. Jackson, Phys. Fluids **2**, 432 (1959); J. Foch and G. W. Ford, in *Studies in Statistical Mechanics,* edited by J. de Boer and G. E. Uhlenbeck (North-Holland, Amsterdam, 1970), Vol. 5.

[32]K. Baldwin (unpublished).

[33]H. L. Störmer, A. C. Gossard, W. Wiegmann, R. Blondel, and K. Baldwin, Appl. Phys. Lett. **44**, 139 (1984).

[34]J. Shah, A. Pinczuk, H. L. Störmer, A. C. Gossard, and W. Wiegmann, Appl. Phys. Lett. **44**, 322 (1984).

[35]W. Walukiewicz, J. Lagowsky, L. Jastrzebski, H. C. Gatos, J. Appl. Phys. **50**, 5040 (1979).

[36]G. E. Stillmann (unpublished).

[37]M. A. Krivov, E. V. Malisova, E. N. Mel'chenko, V. S. Morozov, M. P. Nikiforova, S. S. Khludkov, Yu. A. Grigor'ev, O. L. Egorova, and V. B. Osvenskii, Izv. Vyssh. Uchebn. Zaved. Fiz. **26**, 94 (1983) [Sov. Phys. J. **26**, 1047 (1983)].

[38]*Semiconductors,* Vols. 17a and 17b of *Numerical Data and Functional Relationships in Science and Technology,* Landolt-Börnstein New Series, Group III, edited by O. Madelung, M. Schulz, and H. Weiss (Springer Verlag, Berlin, 1982), p. 531.

[39]R. A. Höpfel, Appl. Phys. Lett. **51**, 106 (1987).

[40]J. Shah, A. Pinczuk, A. C. Gossard, and W. Wiegmann, Phys. Rev. Lett. **54**, 2045 (1985).

[41]E. M. Conwell, *High Field Transport in Semiconductors* (Academic, New York, 1967).

[42]H. Dreicer, Phys. Rev. **117**, 343 (1960).

[43]I. P. Shkarofsky, T. W. Johnston, and M. P. Bachynsky, *The Particle Kinetics of Plasmas* (Addison-Wesley, Reading, Mass., 1966).

[44]M. Combescot and R. Combescot, Phys. Rev. B **35**, 7986 (1987).

[45]M. A. Osman, U. Ravaioli, R. Joshi, W. Pötz, and D. K. Ferry, in *Proceedings of the 18th International Conference on The Physics of Semiconductors,* edited by O. Engström (World Scientific, Singapore, 1987), p. 1311.